Dyes and Pigments 87 (2010) 109–118

Contents lists available at ScienceDirect

Dyes and Pigments

journal homepage: www.elsevier.com/locate/dyepig

The synthesis, structure and photoluminescence of coumarin-based chromophores

Yi-Feng Sun [a,*], Shu-Hong Xu [b], Ren-Tao Wu [a], Zhu-Yuan Wang [b], Ze-Bao Zheng [a], Ji-Kun Li [a], Yi-Ping Cui [b]

[a] Department of Chemistry, Taishan University, Taian 271021, China
[b] Advanced Photonics Center, School of Electronic Science and Engineering, Southeast University, Nanjing 210096, China

ARTICLE INFO

Article history:
Received 2 December 2009
Received in revised form
27 February 2010
Accepted 1 March 2010
Available online 15 March 2010

Keywords:
Coumarin
Azo
Pyrazoline
Crystal structure
Photoluminescence
Quantum chemical calculations

ABSTRACT

Coumarin-based chromophores with azo and pyrazoline moieties were synthesized and their structures and properties elucidated using spectroscopy. The coumarins were luminescent, having solid state emission at wavelengths ranging from 400 to 750 nm, depending on structure. The relationships between the solid state photoluminescence and both chemical and crystal structures are discussed.

1. Introduction

Coumarin derivatives have long been recognized to possess multiple biological activities [1–5], especially antioxidant and anti-inflammatory activities and the coumarin unit can be found in many natural and synthetic drug molecules. Moreover, as an important class of organic heterocyclic dyes, coumarin derivatives exhibit unique photochemical and photophysical properties, which render them useful in a variety of applications such as optical brighteners, laser dyes, non-linear optical chromophores, solar energy collectors, fluorescent labels and probes in biology and medicine, as well as two-photon absorption (TPA) materials [6–12]. More importantly, coumarin dyes have also been used as blue, green and red dopants in organic light-emitting diodes (OLEDs). For example, 10-(2-benzothiazolyl)-1,1,7,7 -tetrainethyl-2,3,6,7-tetrahydro-1H,5H,11H-[1]benzo pyrano[6,7,8-*ij*]quinolizin-11-one (**C-545T**) (Fig. 1), which belongs to the highly fluorescent class of coumarin laser dyes, is one of the best green fluorescent dopants, and has widely been used as a doped green emitter in OLEDs [13–16].

Similarly, pyrazoline derivatives generate strong interest stemming from their broad spectrum of pharmacological activities, including antimicrobial, anticonvulsant, anti-inflammatory, analgesic, anticancer, antitubercular and herbicidal [17,18]. Furthermore, pyrazolines show strong fluorescence and have a high hole-transport efficiency and excellent blue emitting properties. Therefore, pyrazoline derivatives have widely been used as whitening or brightening reagents for synthetic fibers, as fluorescence probes in chemosensors, as fluorescent chemosensors for recognition of transition metal ions, as hole-transport materials in electrophotography and electroluminescence fields [19–22]. For instance, 1,5-diphenyl-3-(1-naphthyl)-2-pyrazoline (**DPNPZ**) (Fig. 1) has a strong blue fluorescence emission, and can be used as an emissive dopant in an electroluminescent (EL) device [23].

On the other hand, azo compounds, while being a well-documented class of commercial dyes, are attracting ever increasing attention in the areas of optical data storage, non-linear optical materials, photoswitches, photoprobes, ink-jet printing, biochemical assays, and photocontrol of biological processes [24–26]. The main reason is that these azo chromophores can undergo light-driven, reversible *trans–cis* isomerisation of the azo bond with concomitant change of the structure, dipole moment and optical properties [27].

In view of the considerable importance of these compounds work, the focus of the current research workers turned towards the synthesis of coumarin derivatives containing an azo or pyrazoline

* Corresponding author. Tel.: +86 538 6715546; fax: +86 538 6715536.
E-mail address: sunyf50@yahoo.com.cn (Y.-F. Sun).

0143-7208/$ – see front matter © 2010 Elsevier Ltd. All rights reserved.
doi:10.1016/j.dyepig.2010.03.003

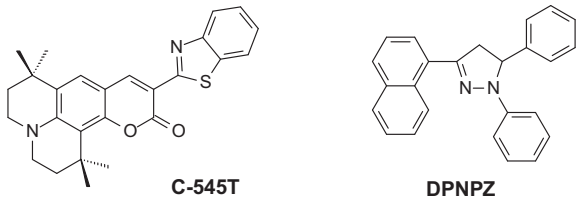

Fig. 1. The structures of C-545T and DPNPZ.

moiety. It was envisaged that compounds containing these moieties in the same molecule may show enhanced biological and optical properties. In previous papers we have reported the synthesis, crystal structures and preliminary spectroscopic properties of various coumarin derivatives [28–30]. However, as the solid state photoluminescence properties of the dyes have not been investigated, in keeping with our interest in the synthesis, crystallography and optical evaluation of coumarin-based chromophores, this paper concerns the synthesis and spectroscopic characterization of novel, coumarin-based chromophores based either on an azo or pyrazoline core. In addition, the photoluminescence properties of the compounds are discussed in the solid state and the structures of **2c** and **4a** were studied both experimentally and theoretically. The synthetic pathway and the structures of target molecules are shown in Figs. 2–4.

2. Experimental

2.1. General

^{1}H NMR spectra were recorded with a Bruker AVANCE-400 or Varian INOVA-600 NMR spectrometer and chemical shifts expressed as δ (ppm) values with TMS as internal standard. The IR spectra were measured on a Nicolet/Nexus-870 FT-IR spectrometer with KBr pellets in the range 4000–400cm^{-1}. Element analysis was taken with a Perkin–Elmer 240 analyzer. Mass spectra (MS) were measured on an LCQ Advantage MAX or VG ZAB-HS mass spectrometer. The melting points were determined with a WRS-1A melting point apparatus and are uncorrected. The Raman spectra were recorded using a Horiba Jobin-Yvon LabRam HR800 Raman microspectrometer, with an excitation laser at 514 nm, and a 600 groove mm^{-1} diffraction grating. Signals were recorded in the range from 200–2500 cm^{-1}. The UV–vis absorption spectra were recorded using a Helios Alpha UV–Vis scanning spectrophotometer. The photoluminescence spectra were measured using a Horiba Jobin-Yvon LabRam HR800 Raman microspectrometer under a 325 nm He–Cd laser excitation. Single crystal was characterized by Bruker Smart 1000 CCD X-ray single crystal diffractometer. All the chemicals are commercially available and they were used without further purification.

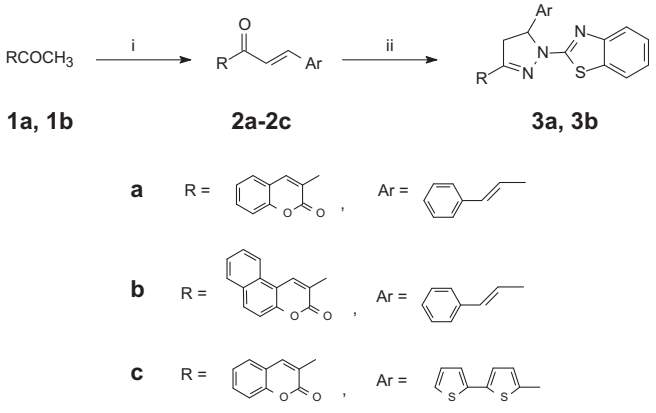

Fig. 2. Synthesis of coumarin–pyrazoline hybrids. Reagents and reaction conditions: (i) ArCHO, Piperidine, EtOH, reflux; (ii) 2-Hydrazino-1,3-benzothiazole, Ethylene glycol, MW.

2.2. Synthesis of the coumarin–chalcone hybrids (*2*)

Three coumarin–chalcone hybrids were synthesized from 3-acetyl coumarins and cinnamaldehyde or 2,2′-bithiophene-5-carbaldehyde in the presence of piperidine in ethanol under microwave irradiation following the method reported previously [28]. 3-((5-Phenyl)pent-2,4-dienoyl)-2*H*-1-naphtho[2,1-*b*]pyran-2-one (**2b**) and 3-(3-(2-(thiophen-2-yl)thiophen-5-yl)prop-2-enoyl)-2*H*-1-benzopyran-2-one (**2c**) have been reported in previous papers [28,31].

2.2.1. 3-((5-Phenyl)pent-2,4-dienoyl)-2H-1-benzopyran-2-one (*2a*)

Recrystallization from ethanol–acetone gave the title compound **2a** as yellow crystals, yield 62%; mp 182–184 °C; ^{1}H NMR (400 MHz, $CDCl_3$/TMS) δ: 7.02–7.10 (m, 2H), 7.31–7.40 (m, 5H), 7.47–7.52 (m, 3H), 7.63–7.70 (m, 3H), 8.56 (s, 1H); IR (KBr) ν: 1732, 1651, 1612, 1574, 1451, 1348, 1232, 1183, 1143, 997, 751, 689, 577 cm^{-1}. Anal. calcd. for $C_{20}H_{14}O_3$: C 79.46, H 4.67; found C 79.25, H 4.74.

2.3. Synthesis of the coumarin–pyrazoline derivatives (*3*)

Two coumarin–pyrazoline derivatives were synthesized from coumarin–chalcone hybrids (**2**) and 2-hydrazino-1,3-benzothiazole in ethylene glycol under microwave irradiation according to the method reported previously [29].

2.3.1. 1-(Benzothiazol-2-yl)-3-(-2-oxo-2H-1-benzopyran-3-yl)-5-styryl-2-pyrazoline (*3a*)

Recrystallization from chloroform gave the title compound **3a** as yellow solid, yield 63%; mp > 240 °C; ^{1}H NMR (400 MHz, $CDCl_3$/TMS) δ: 3.62 (dd, J = 5.6, 18.6 Hz, 1H), 3.98 (dd, J = 11.7, 18.6 Hz, 1H), 5.46–5.53 (m, 1H), 6.41 (dd, J = 6.6, 15.9 Hz, 1H), 6.76 (d, J = 15.9 Hz, 1H), 7.16 (t, J = 7.6 Hz, 1H), 7.24–7.42 (m, 8H), 7.57–7.71 (m, 4H), 8.51 (s, 1H). IR (KBr) ν: 1728, 1601, 1567, 1551, 1533, 1455, 1443, 1360, 1277, 1243, 1139, 1106, 959, 881, 747, 720, 697, 638 cm^{-1}. MS m/z: 450.6 (M + 1). Anal. calcd. for $C_{27}H_{19}N_3O_2S$: C 72.14, H 4.26, N 9.35; found: C 72.38, H 4.61, N 9.13.

2.3.2. 1-(Benzothiazol-2-yl)-3-(-2-oxo-2H-1-naphtho[2,1-b]pyran -3-yl)-5-styryl-2-pyrazoline (*3b*)

Recrystallization from chloroform gave the title compound **3b** as red solid, yield 52%; mp 216 °C (decompose); ^{1}H NMR (600 MHz, $CDCl_3$/TMS) δ: 3.65 (dd, J = 5.4, 18.6 Hz, 1H), 4.02 (dd, J = 11.7, 18.6 Hz, 1H), 5.50–5.53 (m, 1H), 6.41 (dd, J = 6.6, 15.6 Hz, 1H), 6.76 (d, J = 15.6 Hz, 1H), 7.07–8.42 (m,15H), 9.25 (s, 1H). IR (KBr) ν: 1726, 1598, 1568, 1527, 1440, 1281, 1214, 1143, 994, 810, 743, 687 cm^{-1}. MS m/z: 500.2 (M + 1). Anal. calcd. for $C_{31}H_{21}N_3O_2S$: C 74.53, H 4.24, N 8.41; found: C 74.33, H 4.37, N 8.26.

2.4. Synthesis of the coumarin–azo derivatives (*4*)

Azocoumarins were prepared according to the method described earlier [30] which was modified. Aromatic amines (10 mmol) were dissolved in 6 M HCl (8 mL) and diazotised using sodium nitrite (12 mmol in 5 mL of water) solution at 0 °C with stirring. On completion of diazotization (30–40 min), the resulting diazonium salt solution was added dropwise to a cold, alkaline solution of salicylaldehyde (or 3-methoxysalicylaldehyde) (10 mmol) in 2% aq

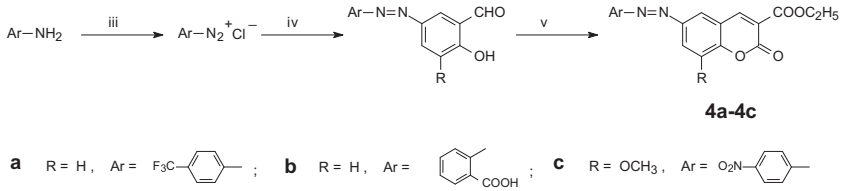

Fig. 3. Synthesis of the coumarine-azo dyes. Reagents and reaction conditions: (iii) $NaNO_2$, HCl, 0–5 °C; (iv) Salicylaldehyde or 3-Methoxysalicylaldehyde, pH = 8–9, 0–5 °C; (v) $CH_2(COOC_2H_5)_2$, EtOH, Piperidine, Glacial acetic acid, reflux.

NaOH solution (50 mL) with stirring. During coupling, the reaction temperature was maintained at 0–5 °C and the pH at 8–9 by the addition of 0.5% aq NaOH solution. On completion of coupling the precipitate was filtered and washed thoroughly with water and dried. The product was further purified by recrystallization from acetone or ethanol.

To a mixture of arylazosalicylaldehydes (5 mmol) and diethyl malonate (5 mmol) in ethanol (20 mL), glacial acetic acid (0.3 mL) and piperidine (0.3 mL) were added under rapid stirring. The reaction mixture was heated under reflux for 5 h and, after cooling, the solid was filtered and recrystallized from a suitable solvent to afford the pure product.

*2.4.1. Ethyl 6-(4-trifluoromethylphenyl)azo-2H-1-benzopyran-2-one-3-carboxylate (**4a**)*

Recrystallization from ethanol gave the title compound **4a** as red crystals, yield 68%; mp 206–208 °C; ^{1}H NMR (600 MHz, $CDCl_3$/TMS) δ: 1.44 (t, J = 6.6 Hz, 3H), 4.45 (q, J = 7.2 Hz, 2H), 7.51 (d, J = 9.0 Hz, 1H), 7.81 (d, J = 7.8 Hz, 2H), 8.03 (d, J = 7.8 Hz, 2H), 8.24 (s, 1H), 8.26 (d, J = 8.4 Hz, 1H), 8.65 (s, 1H). IR (KBr) ν: 1746, 1706, 1614, 1557, 1475, 1322, 1245, 1066, 846, 794, 605 cm^{-1}. FAB-MS m/z: 391 (M + 1). Anal. calcd. for $C_{19}H_{13}F_3N_2O_4$: C 58.47, H 3.36, N 7.18; found: C 58.33, H 3.49, N 7.02.

*2.4.2. Ethyl 6-(2-carboxylphenyl)azo-2H-1-benzopyran-2-one-3-carboxylate (**4b**)*

Recrystallization from acetone gave the title compound **4b** as yellow crystals, yield 52%; mp 214–215 °C; ^{1}H NMR (600 MHz, DMSO-d_6/TMS) δ: 1.33 (t, J = 7.2 Hz, 3H), 4.32 (q, J = 7.2 Hz, 2H), 7.57 (d, J = 7.8 Hz, 1H), 7.62 (t, J = 7.2 Hz, 1H), 7.66 (d, J = 8.4 Hz, 1H), 7.71 (t, J = 7.5 Hz, 1H), 7.83 (d, J = 7.2 Hz, 1H), 8.14 (dd, J = 8.7, 2.7 Hz, 1H), 8.49 (d, J = 2.4 Hz, 1H), 8.95 (s, 1H), 13.19 (s, 1H). IR (KBr) ν: 1742, 1690, 1619, 1562, 1363, 1296, 1250, 1148, 1025, 974, 789, 682, 579 cm^{-1}. FAB-MS m/z: 367 (M + 1). Anal. calcd. for $C_{19}H_{14}N_2O_6$: C 62.30, H 3.85, N 7.65; found: C 62.45, H 3.96, N 7.41.

*2.4.3. Ethyl 8-methoxy-6-(4-nitrophenyl)azo-2H-1-benzopyran-2-one-3-carboxylate (**4c**)*

Recrystallization from ethanol–DMF gave the title compound **4c** as yellow solid, yield 59%; mp 265–266 °C; ^{1}H NMR (600 MHz, $CDCl_3$/TMS) δ: 1.44 (t, J = 7.2 Hz, 3H), 4.09 (s, 1H), 4.45 (q, J = 7.2 Hz, 2H), 7.78 (d, J = 1.8 Hz, 1H), 7.93 (d, J = 1.8 Hz, 1H), 8.07 (d, J = 8.4 Hz, 2H), 8.42 (d, J = 9.0 Hz, 1H), 8.64 (s, 1H). IR (KBr) ν: 1764, 1698, 1612, 1574, 1522, 1471, 1383, 1342, 1246, 1142, 1107, 1026, 964, 878, 810, 692 cm^{-1}. MS m/z: 398.4 (M + 1). Anal. calcd. for $C_{19}H_{15}N_3O_7$: C 57.43, H 3.81, N 10.58; found: C 57.29, H 3.92, N 10.43.

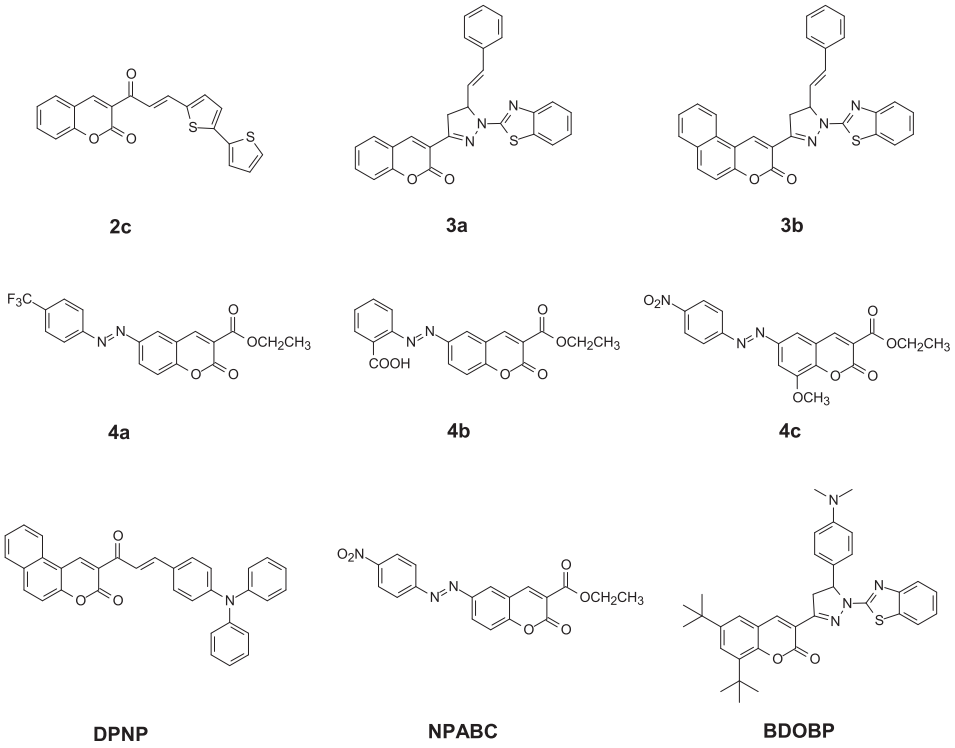

Fig. 4. The structures of the coumarin-based dyes.

2.5. X-ray crystallography

Suitable single crystals of **2c** and **4a** for X-ray structural analysis were obtained by slow evaporation of the ethanol or DMF solutions. The diffraction data for both structures were collected with a Bruker Smart Apex 1000 CCD X-ray single crystal diffractometer using a graphite monochromated Mo Kα radiation ($\lambda = 0.071073$ nm) at 273(2) K. The structures were solved by direct methods with SHELXS-97 program and refinements on F^2 were performed with SHELXL-97 program by full-matrix least-squares techniques with anisotropic thermal parameters for the non-hydrogen atoms. All H atoms were initially located in a difference Fourier map. The methyl H atoms were then constrained to an ideal geometry, with C–H = 0.096 nm and $U_{iso}(H) = 1.5U_{eq}(C)$. All other H atoms were placed in geometrically idealized positions and constrained to ride on their parent atoms with C–H distances 0.093–0.097 nm and $U_{iso}(H) = 1.2U_{eq}(C)$. A summary of the crystallographic data and structure refinement details is given in Table 1.

3. Results and discussion

3.1. Synthesis

Compounds **2** and **3** were prepared using the method reported by us previously [28,29], as depicted in Fig. 2. Claisen–Schmidt condensation of **1** with cinnamaldehyde or 2,2′-bithiophene-5-carbaldehyde yielded the corresponding chalcones **2**. When the chalcones were treated with 2-hydrazino-1,3-benzothiazole in ethylene glycol under microwave irradiation, the pyrazoline derivatives **3** were obtained in 52–63% yield.

The azocoumarins (**4a**–**4c**) were synthesized by condensation of azosalicylaldehydes and diethyl malonate in the presence of glacial acetic acid and piperidine (Fig. 3). The azosalicylaldehydes were prepared by diazotisation of aromatic amines and then a coupling reaction with either salicylaldehyde or 3-methoxysalicylaldehyde.

The structure and purity of the resulting new compounds were confirmed by spectral data and elemental analysis. In the IR spectra of these compounds, the strong bands at around 1726–1764 cm^{-1} confirm the presence of a coumarin skeleton. Comparison of the IR spectrum of **2a** (1732 and 1651 cm^{-1}) with that of compound **3a**

Table 1
Crystal data and structure refinement.

Compound	**2c**	**4a**
Empirical formula	$C_{20}H_{12}O_3S_2$	$C_{19}H_{13}F_3N_2O_4$
Formula weight	364.42	390.31
Temperature (K)	273(2)	273(2)
Crystal system,	Monoclinic	Triclinic
Space group	$P2_1/c$	$P\overline{1}$
Unit cell dimensions		
a (nm)	0.52115 (10)	0.69007 (19)
b (nm)	0.95258 (18)	0.7746 (2)
c (nm)	3.2937 (7)	1.6975 (5)
α (°)	90	88.797 (5)
β (°)	91.797 (3)	81.253 (4)
γ (°)	90	73.407 (4)
Volume (nm^3), Z	1.6343 (6), 4	0.8592 (4), 2
D_{calc} (Mg/m^3)	1.481	1.509
Absorption coefficient (mm^{-1})	0.342	0.128
F (0 0 0)	752	400
Crystal size (mm)	0.21 × 0.16 × 0.12	0.21 × 0.16 × 0.12
θ range for data collection (°)	2.23 to 25.05	2.43 to 25.05
Limiting indices	$-6 \le h \le 6$	$-8 \le h \le 7$
	$-8 \le k \le 11$	$-9 \le k \le 8$
	$-37 \le l \le 39$	$-20 \le l \le 17$
Reflections collected/unique	8385/2879	4534/3016
	[$R_{int} = 0.0284$]	[$R_{int} = 0.0190$]
Max. and min. transmission	0.9601 and 0.9316	0.9848 and 0.9736
Data/restraints/parameters	2879/0/227	3016/0/254
Goodness-of-fit on F^2	1.040	1.057
Final R indices [$I > 2$sigma (I)]	$R_1 = 0.0403$;	$R_1 = 0.0601$;
	$wR_2 = 0.0955$	$wR_2 = 0.1756$
R indices (all data)	$R_1 = 0.0616$;	$R_1 = 0.0694$;
	$wR_2 = 0.1089$	$wR_2 = 0.1881$
Extinction coefficient	0.0037 (7)	0.047 (7)
Largest diff. peak and hole (e nm^{-3})	197 and −328	692 and −413
CCDC	750 904	750 905

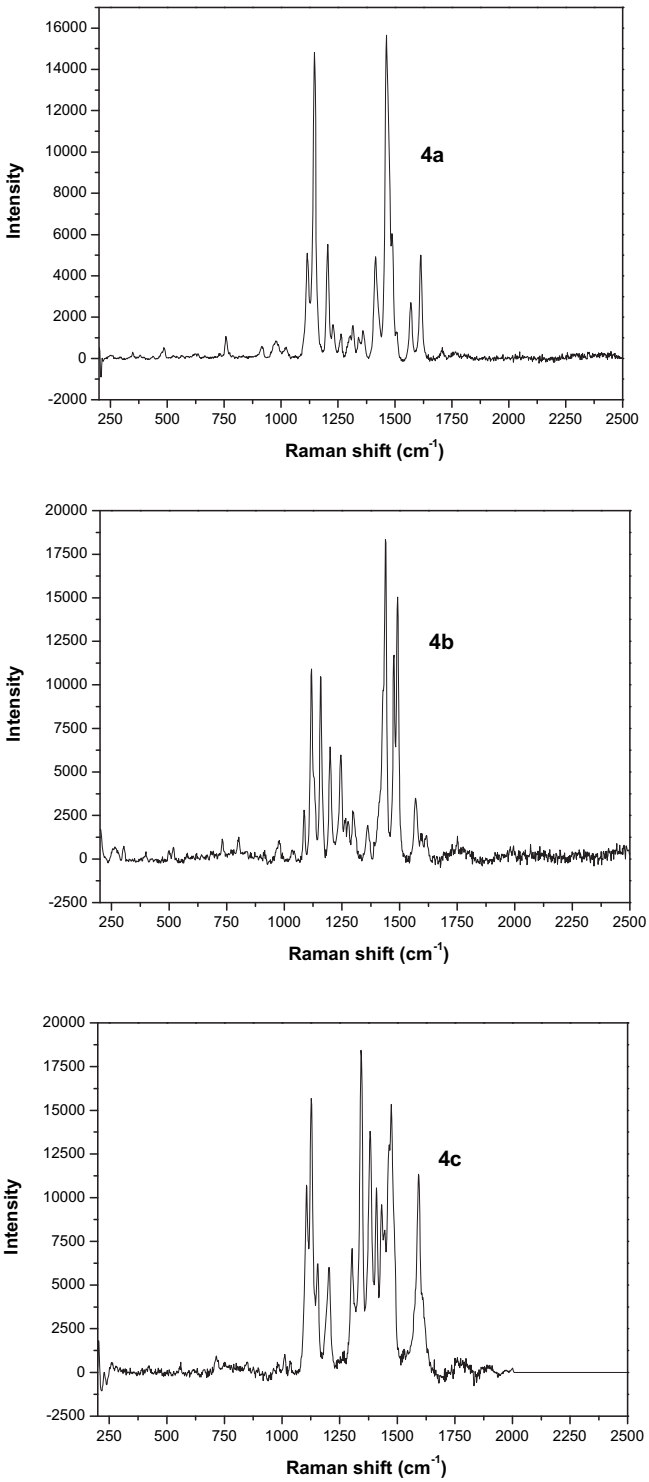

Fig. 5. Raman spectra of the coumarin-azo dyes (**4a**–**4c**).

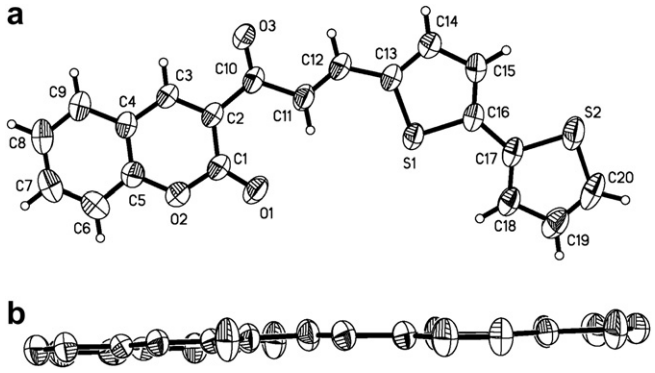

Fig. 6. (a) The molecular structure of **2c**, showing the atom-labelling scheme. Displacement ellipsoids are drawn at the 50% probability level. H atoms are shown as small spheres of arbitrary radius. (b) The side elevation of **2c**. H atoms are omitted for clarity.

clearly indicated the absence of a band around 1651 cm^{-1} due to C═O of chalcone, which clearly confirmed that a cyclo-condensation with 2-hydrazino-1,3-benzothiazole had taken place. In the case of **4c**, the IR spectra show two strong bands located around 1522 and 1342 cm^{-1}, which can be ascribed to the presence of the $-NO_2$ group.

The Raman spectra of the solid samples of these compounds (**2**, **3** and **4**) have been measured. However, unfortunately, among these molecules, the Raman spectra of compounds **2** and **3** cannot be obtained due to their strong fluorescence interference. The Raman spectra of **4** are shown in Fig. 5. Generally, in the Raman spectra, ν(N═N) is normally a quite intense single peak, compared with the extremely weak corresponding band in the IR [32]. Thus, in the Raman spectrum, the corresponding band (ν(N═N)) is more easily recognized by its high intensity, which is due to the large polarizability derivative associated with the N═N stretch. Obviously, all three azocoumarin derivatives have a strong band (ν(N═N)) in the region 1439–1475 cm^{-1} as shown in Fig. 5. The strong Raman activity of ν(N═N) in this series of compounds suggests that Raman spectroscopy is a preferred means of identifying ν(N═N) in azo systems, especially in view of the difficulty in distinguishing ν (N═N) from aromatic absorptions in the IR. Additionally for compound **4c**, the vibration of the $-NO_2$ group seen at 1342 cm^{-1} in the IR spectrum appears at 1343 cm^{-1} in the Raman spectrum as a strong band.

The structures of the prepared compounds were also confirmed by ^{1}H NMR spectroscopy. The ^{1}H NMR spectra of these coumarin dyes show a clearly distinguishable intense singlet at $\delta = 8.51–9.25$ ppm for H-4 of the coumarin nucleus. Such a signal is characteristic for coumarin system protons [33].

In the ^{1}H NMR spectra of compounds **3** signals of the CH_2–CH fragment of the pyrazoline ring were present. These protons appear as two doublets of doublets and a multiplet, respectively, at the $\delta = 3.58–3.68$, 3.94–4.04 and 5.46–5.53 ppm regions, integrating for one proton each. Moreover, the ^{1}H NMR spectra also exhibited the presence of two *trans*-olefinic protons at δ 6.41 and 6.76 ($J = 15.6–15.9$ Hz).

Additionally, the azocoumarins **4b** and **4c** gave a characteristic doublet at δ 7.93–8.49, which was assigned to H-5 of the coumarin nucleus, while the corresponding C-5 proton in **4a** appeared as a singlet at δ 8.24. For compound **4b** a characteristic carboxyl proton singlet at δ 13.19 was apparent in the ^{1}H NMR spectrum.

3.2. Crystal structure

Although compound **2c** has been studied previously by us [28], the crystal structure of **2c** has not been reported. So, in order to study the structure–property relationship, its crystal structure was elucidated. The crystal structure of **2c** is shown in Fig. 6. For **2c** the coumarin ring and 2,2′-bithiophene ring system are essentially planar with maximum deviations of 0.00282 and 0.00402 nm for atoms C1 and S2, respectively. The dihedral angle between the 2,2′-bithiophene ring plane and the ring plane of coumarin is 5.0°, which indicates that the whole molecule is nearly planar (Fig. 6). This is in marked contrast to the orientations in 3-(3-(4-*N*,*N*-diphenyl aminophenyl)prop-2-enoyl) -2*H*-1-naphtho[2,1-*b*]pyran-2-one (**DPNP**) (Fig. 4), which were previously reported by us [28], in which three phenyl rings all are rotated significantly out of the plane of the rest of the molecule.

In addition, molecule **2c** adopts a *trans* configuration about the central olefinic bond, as in **DPNP**. Moreover, the linkage between the 3-actylcoumarin system and 2,2′-bithiophene ring system with bond lengths of C10–C11: 0.1465(3) nm, C11–C12: 0.1321 (3) nm and C12–C13: 0.1440(3) nm, suggests that all non-hydrogen atoms between donor (2,2′-bithiophene ring system)

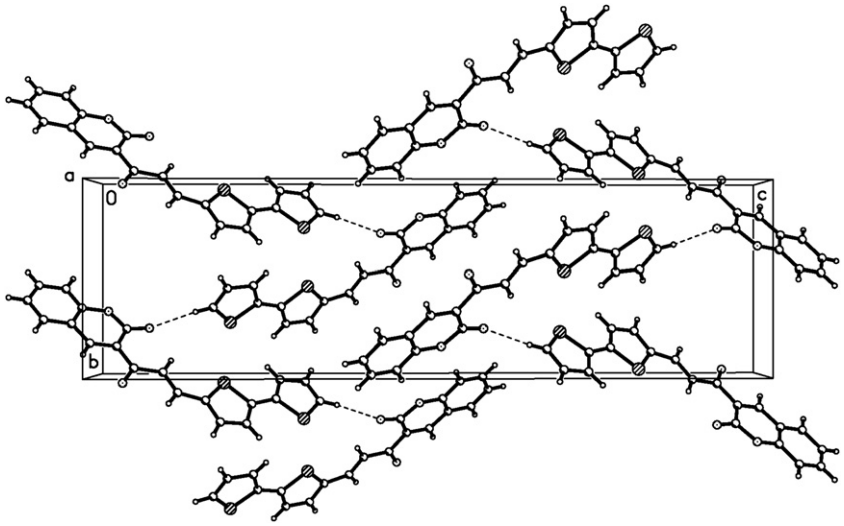

Fig. 7. The chain structure formed *via* hydrogen bonds in **2c**. The dashed lines indicate hydrogen bonds.

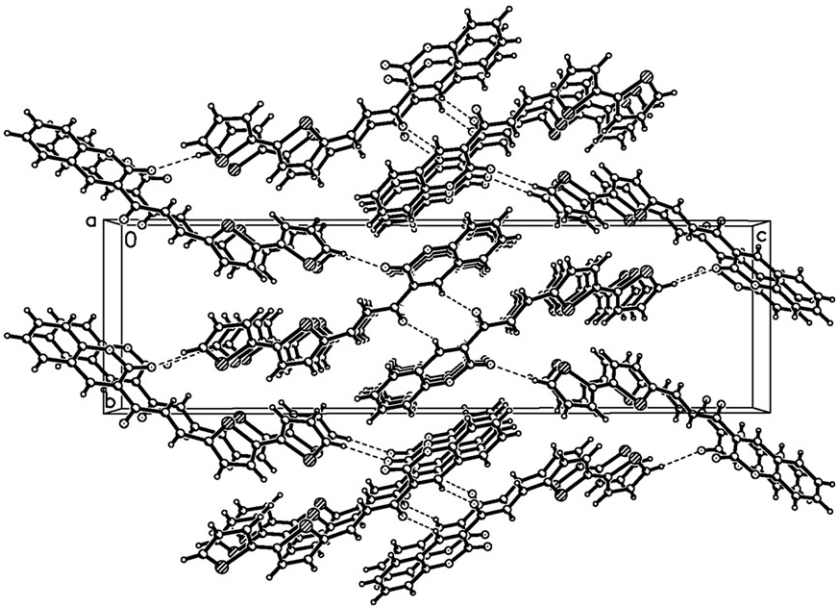

Fig. 8. A packing diagram for **2c**, viewed down the *a* axis.

and acceptor (3-carbonylcoumarin system) are highly conjugated, leading to a π-bridge for the charge transfer from the 2,2′-bithiophene ring system to 3-carbonylcoumarin system. These characteristics are in good agreement with those of **DPNP**.

Meanwhile, the molecules are linked together by the weak intermolecular C–H…O hydrogen bonds (C20–H20…O1: C–H = 0.093 nm, H20…O1 = 0.2432 nm, C20…O1 = 0.3356(3) nm, C20–H20…O1 = 172°) into a one dimensional *zigzag* chain running along the *b*-axis (Fig. 7), which are cross-linked into a two-dimensional framework by the weak intermolecular C–H…O hydrogen bonds (C3–H3…O3^{i}: C–H = 0.093 nm, H3…O3 = 0.2556 nm, C3…O3 = 0.3405(3) nm, C3–H3…O3 = 152°; symmetry code: (i) 2 − *x*, 2 − *y*, −*z*;). Another interesting feature of the intermolecular interaction may be π–π stacking interactions between molecules in the crystal lattice. As a result, the molecules are further self-assembled to form an extended network structure (Fig. 8).

In **4a** although the coumarin moiety is essentially planar, the coumarin and phenyl rings, which adopt a distorted *trans* configuration about the N=N double-bond, are not coplanar with a dihedral angle of 43.1°. As a result, the whole compound is not a planar molecule (Fig. 9). Moreover, the N1=N2 bond length of 0.1250(3) nm is indicative of double-bond character. Similar geometry has been observed in related azo dye ethyl 6-(4-nitrophenyl)azo-2*H*-1-benzopyran-2-one-3-carboxylate (**NPABC**) (Fig. 4), which were reported previously by us [30]. But compared with **4a**, the two ring systems in **NPABC** is almost coplanar and form a dihedral angle of 3.7°. Thus, the significant deviation from coplanarity in **4a** might be attributed to the presence of the fairly bulky *p*-trifluoromethyl moiety.

Additionally, the weak intermolecular C–H…O hydrogen bonds (C17–H17…O2^{ii}: C–H = 0.093 nm, H17…O2 = 0.2369 nm,

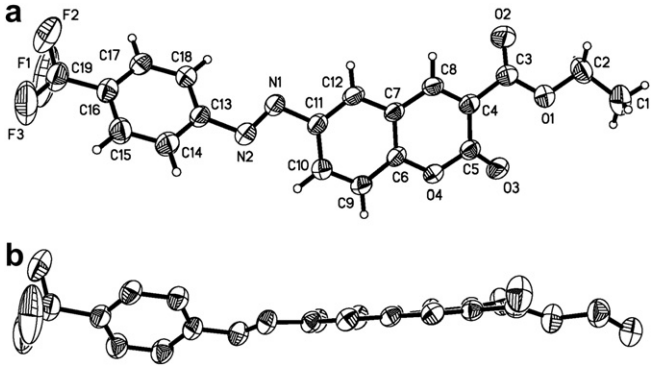

Fig. 9. (a) The molecular structure of **4a**, showing the atom-labelling scheme. Displacement ellipsoids are drawn at the 50% probability level. H atoms are shown as small spheres of arbitrary radius. (b) The side elevation of **4a**. H atoms are omitted for clarity.

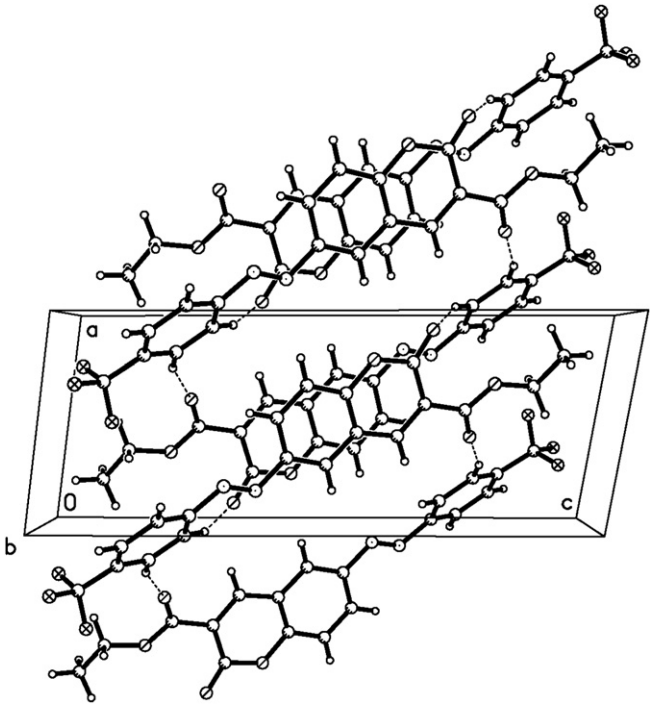

Fig. 10. The one dimensional structure formed *via* hydrogen bonds in **4a**. The dashed lines indicate hydrogen bonds.

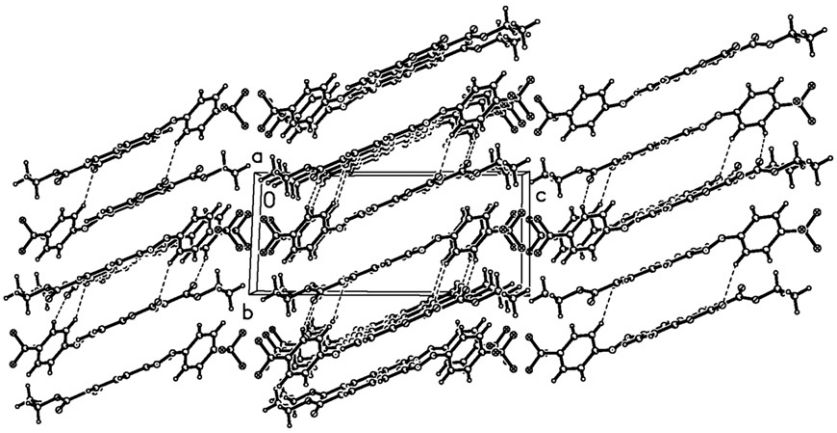

Fig. 11. A packing diagram for **4a**, viewed down the *a* axis.

C17…O2 = 0.3256(3) nm, C17–H17…O2 = 159°; C18–H18…O3^{iii}: C–H = 0.093 nm, H18…O3 = 0.2513 nm, C18…O3 = 0.3382(3) nm, C18–H18…O3 = 156°; symmetry code: (ii) $2-x, 2-y, 1-z$; (iii) $1-x, 2-y, 1-z$) are also observed in the structure. The molecules are linked together by such intermolecular hydrogen bonds into a one dimensional structure extending along the *a* axis (Fig. 10), which are further held together *via* π–π stacking interactions to form a two-dimensional supramolecular architecture. Finally, the molecules are assembled to form a layer structure (Fig. 11).

The formation of ordered structures from the dyes **2c** and **4a** is expected to have a potentially large impact on their optoelectronic properties in the solid state.

3.3. UV–Vis absorption spectra

The structures of the target molecules are shown in Fig. 4. As seen from Fig. 4, for two coumarin–pyrazolines, **3a** and **3b**, structural modification occurs only in one terminal unit, where a coumarin moiety was replaced by a benzocoumarin system. On the other hand, three molecules **4a**–**4c** contain both a coumarin core and an azo group. These molecules are related, but their chemical structures are differentiated by introduction of various substituents.

UV–vis absorption spectra of these molecules in diluted chloroform solutions (2×10^{-5} M) are given in Fig. 12. Compound **2a** shows a sharp absorption peak at 375 nm with a shoulder at 315 nm. The two coumarin–pyrazolines (**3a** and **3b**) have similar absorption spectra, and three sharp absorption peaks located at 264, 294 and 421 nm, are observed. The first absorption band (λ_{max} = 421 nm) of pyrazoline **3a** exhibits a red-shift of 46 nm compared to that of **2a** (λ_{max} = 375 nm), which further confirmed the formation of pyrazoline ring system. However, compared with **3a**, a shoulder peak around 470 nm on the longer wavelength side of the main peak is clearly evident in **3b**. It is well known that pyrazoline compounds are typical intra-molecular charge transfer compounds [23,27]. Thus, this difference might be attributed to the larger conjugation for benzocoumarin relative to coumarin system. Additionally it is noted that λ_{max} (421 nm) of the first absorption band of pyrazoline **3a** is very close to that of 1-(benzothiazol-2-yl)-3-(6,8-di-tert-butyl -2-oxo-2*H*-1-benzopyran-3-yl)-5-(4-*N*,*N*-dimethylaminophenyl)-2-pyrazoline (**BDOBP**) (Fig. 4) (λ_{max} = 423 nm), reported by us previously [29], owing to their very similar structure.

Compound **4b** exhibits absorption spectral features that are similar to those of **4c** with two major absorption bands at around 314 and 362 nm. But, in the case **4a**, only one sharp absorption peak appears around 305 nm with a shoulder towards longer wavelength, and exhibits a blue-shift of 2–9 nm compared with the corresponding peaks that of **4b** and **4c**. The results above imply that less π-electrons and shorter π-conjugated structure may be involved in **4a** than those in **4b** and **4c**.

3.4. Photoluminescence spectra

The photoluminescence (PL) of coumarin dyes were examined with a He–Cd laser of 325 nm at room temperature. To probe the relationship between structure and spectral properties, the photoluminescence of **2c** is also discussed for comparative purposes (Fig. 13). The coumarin dyes **3** and **4** exhibit different emission colors when in the solid state, as shown in Fig. 14. The solid PL spectrum for **2c** exhibits (Fig. 13) three primary color emission bands, a strong narrow blue emission at 404 nm and a strong green emission at 524 nm, as well as a broad red emission at 697 nm (Fig. 13(b)). These PL spectral characteristics are similar to those observed in the corresponding chloroform solution of **2c** (Fig. 13 (a)), in which the three corresponding emission bands were located at 420, 534 and 737 nm, respectively. Noticeably, in the solid state case we did not observe the splitting of the blue band, which was noted for the chloroform solution. A blue-shift of about 10–40 nm in the blue, yellow and red emission maximum is observed from solution to solid state.

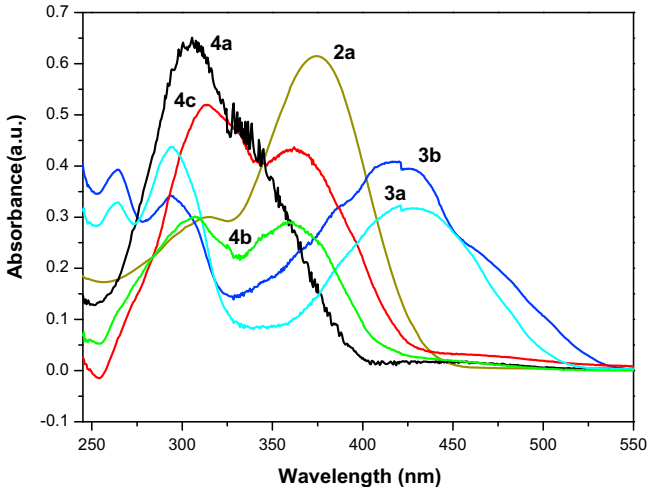

Fig. 12. Absorption spectra of the coumarin-based dyes in chloroform solution.

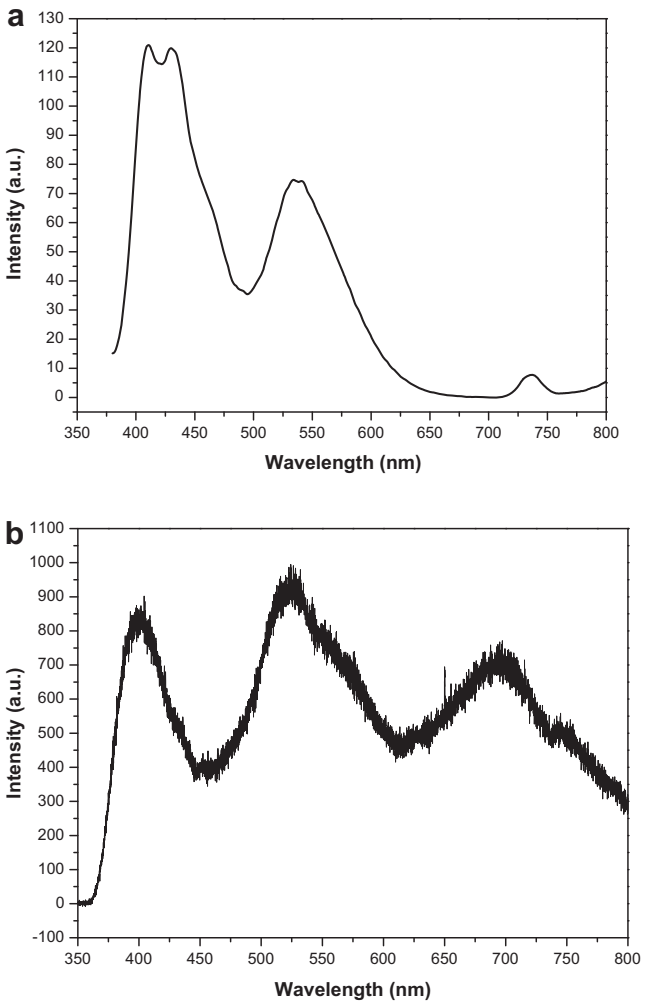

Fig. 13. PL spectra of **2c** in chloroform solution (a) and in the solid state (b).

Such results may be due to the fact that the PL spectrum of a luminescent molecule in dilute solution reflect mainly its single molecular characteristic, while the PL spectrum of the same luminescent molecule in an organic crystal results from the interaction of large numbers of molecules. So, in a crystal of **2c**, the blue-shifts of the emission peaks possibly result from the strong interactions between molecules of **2c**. The presence of the intermolecular interactions have been demonstrated by X-ray diffraction crystal structure analysis in this work. As mentioned above, the crystal structure analysis results reveal that **2c** is nearly planar, and the main driving forces in the formation of the extended network structure are intermolecular hydrogen bonding and π–π stacking interactions. Consequently, crystal **2c** with interchromophore interactions displays the blue-shifts of the PL peaks, especially the red band, which was enhanced, broadened and blue-shifted up to 40 nm compared to that in chloroform solution.

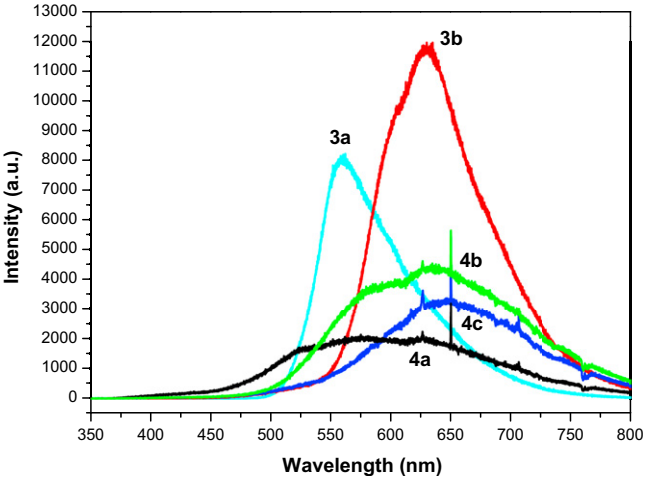

Fig. 14. Solid state PL spectra of the coumarin-based dyes.

In contrast, only an emission peak could be observed in the photoluminescence spectra of molecules **3** (Fig. 14), which indicates that the emission occurs from the lowest excited state with the largest oscillator strength. Compound **3a** shows a yellow emission band centered at 562 nm while **3b** displays a specific red emission band centered at 635 nm. The emission peak of **3b** is significantly shifted to longer wavelength with respect to that of **3a**, and both exhibit red-shifted emission as compared to **BDOBP** (λ_{max} = 529 nm) [29].

The three azocoumarins **4a**–**4c** have very similar photoluminescence spectra, and present a broad emission band with the shoulder peak centered in the 590–650 nm wavelength region, the maximum emission peaks undergo a red-shift from **4a** (580 nm) to **4b** (640 nm), and to **4c** (650 nm). Obviously, the maximum emission peak of **4b** is red-shifted by 60 nm, when compared to **4a**, but blue-shifted by about 10 nm with respect to that of **4c**. It should be noted that compound **4a** has a very broad emission band spanning the entire visible spectrum from 400 to 750 nm, which can be attributed to intermolecular interactions within the crystal of **4a**.

3.5. Quantum chemical calculations

To gain a deeper insight into the electronic and luminescent properties of **2c**, we performed quantum chemical calculations. The geometry structure of **2c** was optimized at the *ab initio* Hartree–Fock (HF) level with the standard 3-21G basis set (HF/3-21G), all structure optimizations and energy calculations were performed with the GAUSSIAN 98 program. The optimal structure of **2c** is depicted in Fig. 15.

It was found that the calculated results are very close to the experimental values obtained from the X-ray single crystal diffraction. As described above, in crystal structures, molecule of **2c** is nearly planar with a dihedral angle of 5.0° between the coumarin ring and 2,2-bithiophene ring system. The HF calculations predict the planar arrangement of the two ring systems for **2c**, reflecting the strong conjugation across the 3-carbonylcoumarin acceptor group. The reason for the slight discrepancy is probably that theoretical results belong to the isolated molecule and the experimental values are attributed to the molecule in solid state. The geometry of the solid state structure is subject to intermolecular

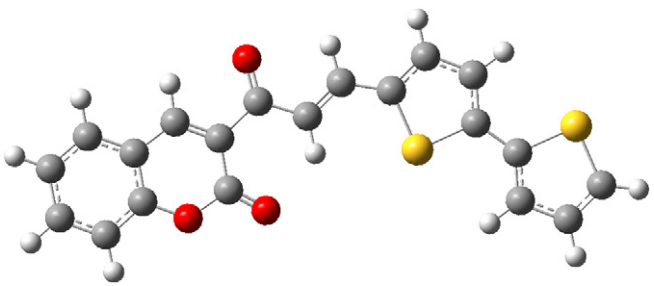

Fig. 15. Optimized structure of **2c** by HF/3-21G method.

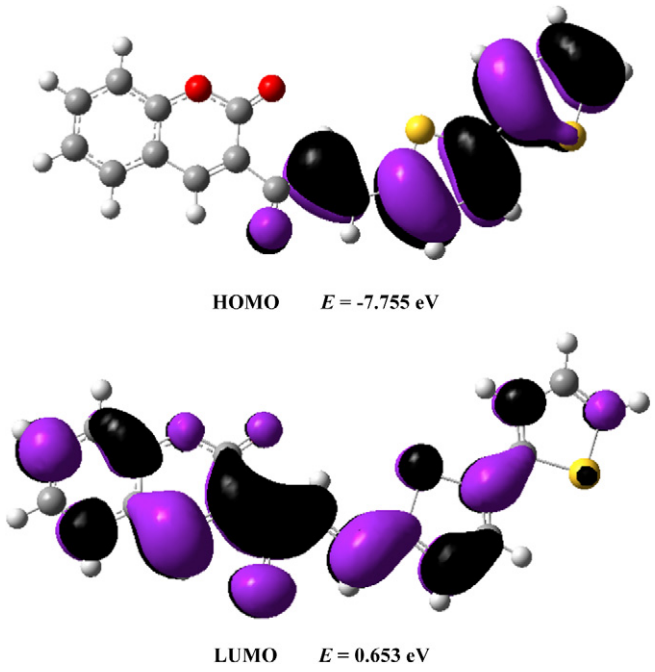

Fig. 16. Molecular orbital surface and energies of the main frontier molecular orbitals for **2c**.

forces, such as van der Waals interactions, crystal packing forces and hydrogen bond forces [34]. Although there is a slight difference between the calculated and experimental values, the general qualitative conclusion drawn from our calculations is consistent with the experimental one.

In an effort to find some clues about the experimental results, The highest occupied molecular orbital (HOMO) and lowest unoccupied molecular orbital (LUMO) energy levels diagrams of dye **2c** are also calculated to check the smooth transfer of electron density when the dye is excited by light. HOMO and LUMO levels of **2c** are shown in Fig. 16.

Generally, the energy values of LUMO and HOMO and their energy gap reflect the chemical activity of the molecule. HOMO as an electron donor represents the ability to donate an electron, while LUMO as an electron acceptor represents the ability to obtain an electron. The smaller the LUMO and HOMO energy gaps, the easier it is for the HOMO electrons to be excited [35].

As shown in Fig. 16, the HOMO and LUMO diagrams of **2c** are likely to secure the efficient electron transfer from the 2,2-bithiophene region of the HOMO to the 3-carbonylcoumarin region of the LUMO (Fig. 16) if electronic transitions occur. The HOMO, for compound **2c**, is localized on 2,2-bithiophene ring system while the LUMO is mainly located on the 3-carbonylcoumarin moiety. Therefore, when electrons transfer from HOMO to LUMO, the electron density significantly decreases in electron donating group 2,2-bithiophene ring system, accompanied by the increase of the electron density in the electron accepting group 3-carbonylcoumarin moiety, indicating that electrons transfer from 2,2-bithiophene ring system to 3-carbonylcoumarin group.

The energies of the HOMO and LUMO for compound **2c** based on the optimized structure are computed at −7.755 and 0.653 eV, respectively. The HOMO–LUMO energy gap for compound **2c** is 8.408 eV. The calculated HOMO and LUMO energies clearly show that charge transfer occurs within the molecule and the optical HOMO–LUMO transition should have a charge-transfer nature. These findings are important for the better understanding of its UV–Vis absorption and PL properties.

4. Conclusions

In summary, we have described the synthesis and detailed characterization of some organic chromophores based on the coumarin moiety. The PL spectra of these molecules are discussed in the solid state. The resulting coumarins cover the emission region from 370 to 750 nm, depending on the effective conjugation length of chromophores. Significantly, the solid state PL spectrum for **2c** exhibits three primary color emission bands, having maxima at 404, 524, and 697 nm, respectively, roughly corresponding to blue, greenish blue, and red light. To the contrary, **4a** displays a quite different PL spectrum, which exhibits a very broad emission band spanning the entire visible spectrum from 400 to 750 nm. X-ray structural analysis show **2c** to be monoclinic, space group $P2_1/c$, while **4a** is triclinic, space group $P\bar{1}$. At the same time, the molecular structure of **2c** is optimized using HF/3-21G and the HOMO and LUMO levels are deduced.

The coumarins are extremely variable in structure, due to the various types of substituents in their basic structure, which can influence their optical properties. Thus, the totality of the results suggests that this system might be effective for the development of long wavelength emissive and white-light-emitting chromophores, and the coumarins are promising candidates for applications in molecular electronics and biological imaging. Our work is currently focused on the further development of these coumarin systems.

Supplementary material

The crystallographic data (excluding structure factors) of **2c** and **4a** have been deposited with the Cambridge Crystallographic Center as supplementary publication no. 750904 and 750 905. Copy of this information may be obtained free of charge *via* www: http://www.ccdc.cam.ac.uk or from The Director, CCDC, 12 Union Road, Cambridge CB221EZ, UK (fax: +44 1223/336 033; email: deposite@ccdc.cam.ac.uk). Structural factors are available on request from the authors.

Acknowledgements

This project was supported by the National Natural Science Foundation of China (No. 60877024 and 60708024) and the Foundation of Taishan University (No. Y04-2-02).

References

[1] Matos MJ, Vina D, Queaada E, Picciau C, Delogu G, Orallo F, et al. A new series of 3-phenylcoumarins as potent and selective MAO-B inhibitors. Bioorganic & Medicinal Chemistry Letters 2009;19:3268–70.
[2] Kostova I. Synthetic and natural coumarins as cytotoxic agents. Current Medicinal Chemistry – Anti-Cancer Agents 2005;5:29–46.
[3] Kontogiorgis CA, Hadjipavlou-Litina DJ. Synthesis and antiinflammatory activity of coumarin derivatives. Journal of Medicinal Chemistry 2005;48(20):6400–8.
[4] Lee S, Sivakumar K, Shin WS, Xie F, Wang Q. Synthesis and anti-angiogenesis activity of coumarin derivatives. Bioorganic & Medicinal Chemistry Letters 2006;16(17):4596–9.
[5] Hamdi N, Puerta MC, Valerga P. Synthesis, structure, antimicrobial and antioxidant investigations of dicoumarol and related compounds. European Journal of Medicinal Chemistry 2008;43:2541–8.
[6] Kim TK, Lee DN, Kim HJ. Highly selective fluorescent sensor for homocysteine and cysteine. Tetrahedron Letters 2008;49:4879–81.
[7] Melavanki RM, Kusanur RA, Kulakarni MV, Kadadevarmath JS. Role of solvent polarity on the fluorescence quenching of newly synthesized 7,8-benzo-4-azidomethyl coumarin by aniline in benzene–acetonitrile mixtures. Journal of Luminescence 2008;128:573–7.
[8] Fu Q, Cheng LL, Zhang Y, Shi WF. Preparation and reversible photo-cross-linking/photo-cleavage behavior of 4-methylcoumarin functionalized hyperbranched polyester. Polymer 2008;49:4981–8.
[9] Yu TZ, Zhang P, Zhao YL, Zhang H, Meng J, Fan DW. Synthesis and photoluminescent properties of two novel tripodal compounds containing coumarin

moieties. Spectrochimica Acta Part A: Molecular and Biomolecular Spectroscopy 2009;73:168–73.
[10] Turki H, Abid S, Fery-Forgues S, Gharbi RE. Optical properties of new fluorescent iminocoumarins: part 1. Dyes and Pigments 2007;73:311–6.
[11] Kim HM, Fang XZ, Yang PR, Yi JS, Ko YG, Piao MJ, et al. Design of molecular two-photon probes for in vivo imaging. 2H-Benzo[h]chromene-2-one derivatives. Tetrahedron Letters 2007;48:2791–5.
[12] Li X, Zhao YX, Wang T, Shi MQ, Wu FP. Coumarin derivatives with enhanced two-photon absorption cross-sections. Dyes and Pigments 2007;74:108–12.
[13] Culligan SW, Chen ACA, Wallace JU, Klubek KP, Tang CW, Chen SH. Effect of hole mobility through emissive layer on temporal stability of blue organic light-emitting diodes. Advanced Functional Materials 2006;16:1481–7.
[14] Hsu SF, Lee CC, Hwang SW, Chen HH, Chen CH, Hu AT. Color-saturated and highly efficient top-emitting organic light-emitting devices. Thin Solid Films 2005;478:271–4.
[15] Hung LS, Chen CH. Recent progress of molecular organic electroluminescent materials and devices. Materials Science and Engineering: R: Reports 2002;39:143–222.
[16] Kim MS, Lim JT, Jeong CH, Lee JH, Yeom GH. White organic light-emitting diodes from three emitter layers. Thin Solid Films 2006;515:891–5.
[17] Manna K, Agrawal YK. Microwave assisted synthesis of new indophenazine 1,3,5-trisubstruted pyrazoline derivatives of benzofuran and their antimicrobial activity. Bioorganic & Medicinal Chemistry Letters 2009;19:2688–92.
[18] Amr AEE, Abdel-Latif NA, Abdalla MM. Synthesis of some new testosterone derivatives fused with substituted pyrazoline ring as promising 5α-reductase inhibitors. Acta Pharmaceutica 2006;56:203–18.
[19] Bai G, Li JF, Li DX, Dong C, Han XY, Lin PH. Synthesis and spectrum characteristic of four new organic fluorescent dyes of pyrazoline compounds. Dyes and Pigments 2007;75:93–8.
[20] Wei XQ, Yang G, Cheng JB, Lu ZY, Xie MG. Synthesis of novel light-emitting calix[4]arene derivatives and their luminescent properties. Optical Materials 2007;29:936–40.
[21] Wang PF, Onozawa-Komatsuzaki N, Himeda Y, Sugihara H, Arakawa H, Kasuga K. 3-(2-Pyridyl)-2-pyrazoline derivatives: novel fluorescent probes for Zn^{2+} ion. Tetrahedron Letters 2001;42:9199–201.
[22] Bian B, Ji SJ, Shi HB. Synthesis and fluorescent property of some novel bis-chromophore compounds containing pyrazoline and naphthalimide groups. Dyes and Pigments 2008;76:348–52.
[23] Zhang XH, Wu SK, Gao ZQ, Lee CS, Lee ST, Kwong HL. Pyrazoline derivatives for blue color emitter in organic electroluminescent devices. Thin Solid Films 2000;371:40–6.
[24] Pavlovic G, Racane L, Cicak H, Tralic-Kulenovic V. The synthesis and structural study of two benzothiazolyl azo dyes: X-ray crystallographic and computational study of azo–hydrazone tautomerism. Dyes and Pigments 2009;83:354–62.
[25] Yager KG, Barrett CJ. Novel photo-switching using azobenzene functional materials. Journal of Photochemistry and Photobiology A: Chemistry 2006;182:250–61.
[26] Feringa BL, Jager WF, de Lange B. Organic materials for reversible optical data storage. Tetrahedron 1993;49:8267–310.
[27] Ji M, Lu R, Bao CY, Xu TH, Zhao YY. Fluorescence modulation in azobenzene-substituted triphenyl pyrazoline derivative. Optical Materials 2004;26:85–8.
[28] Sun YF, Cui YP. The synthesis, characterization and properties of coumarin-based chromophores containing a chalcone moiety. Dyes and Pigments 2008;78:65–76.
[29] Sun YF, Cui YP. The synthesis, structure and spectroscopic properties of novel oxazolone-, pyrazolone- and pyrazoline-containing heterocycle chromophores. Dyes and Pigments 2009;81:27–34.
[30] Sun YF, Song HC, Sun XZ, Xu ZL. Synthesis and structural characterization of new 3-substituted-6-arylazocoumarins. Chinese Journal of Organic Chemistry 2003;23(2):162–6.
[31] Sun YF, Xu YM, Liang HF, Zhang DD, Lu JR, Pan WL, et al. Synthesis and preliminary optical study of coumar in derivatives. Acta Scientiarum Naturalium Universitatis Sunyatseni 2007;46(2):55–8.
[32] Rayner-Canham GW, Sutton D. Identification of ν(N=N) in metal arylazo complexes: the infrared and Raman spectra of some arylazo complexes of rhodium(III). Canadian Journal of Chemistry 1971;49:3994–6.
[33] Hepworth JD, Gabbutt CD, Heron BM. Comprehensive heterocyclic chemistry II: pyrans and their benzo derivatives: structure, vol. 5. Amsterdam: Elsevier; 1996. pp. 301–350.
[34] Zhao PS, Shao DL, Zhang J, Wei Y, Jian FF. Experimental and theoretical studies on a thiocarbamide derivative containing schiff base groups. Bulletin of the Korean Chemical Society 2009;30(7):1667–70.
[35] Riahi S, Eynollahi S, Ganjali MR. Calculation of standard electrode potential and study of solvent effect on electronic parameters of anthraquinone-1-carboxylic acid. International Journal of Electrochemical Science 2009;4:1128–37.